This manuscript has been submitted for publication in Comptes Rendus Geosciences. Please note that the manuscript has yet been accepted for publication.

Rapid response to the M_w 4.9 earthquake of November 11, 2019 in Le Teil, Lower Rhône Valley, France

Cécile Cornou[1], Jean-Paul Ampuero[2], Coralie Aubert[1], Laurence Audin[1], Stéphane Baize[3], Jérémy Billant[2], Florent Brenguier[1], Mathieu Causse[1], Mohamed Chlieh[1], Andy Combey[1], Marcello de Michele[4], Bertrand Delouis[2], Anne Deschamps[2], Matthieu Ferry[5] , Michalis Foumelis[4], Bérénice Froment[3], Céline Gélis[3], Raphaël Grandin[6], Jean-Robert Grasso[1], Estelle Hannouz[1], Sébastien Hok[3], Axel Jung[1], Romain Jolivet[7], Mickaël Langlais[1], Philippe Langlaude[8], Christophe Larroque[2], Philippe Hervé Leloup[9], Kevin Manchuel[10], Léo Marconato[9], Christophe Maron[2], Emmanuel Mathot[11], Emeline Maufroy[1], Diego Mercerat[8], Marianne Metois[12], Emmanuelle Neyman[10], Ildut Pondaven[1], Ludmila Provost[3], Julie Régnier[8], Jean-François Ritz[5], Diane Rivet[2], Antoine Schlupp[13], Anthony Sladen[2], Christophe Voisin[1], Andrea Walpersdorf[1], David Wolynieck[1], Pascal Allemand[9], Elise Beck[14], Etienne Bertrand[8], Véronique Bertrand[15], Pierre Briole[7], Didier Brunel[2], Olivier Cavaillé[2], Jérôme Chèze[2], Françoise Courboulex[2], Isabelle Douste-Bacque[1], Rémi Dretzen[15], Tiziano Giampietro[2], Maxime Godano[2] , Philippe Grandjean[9], Marc Grunberg[15], Gauthier Guerin[2], Stéphane Guillot[1], Elias El Haber[1], Alain Hernandez[15], Hervé Jomard[3], Cécile Lasserre[9], Chao Liang[2], Itzhak Lior[2], Xavier Martin[2] , Daniel Mata[2], Marine Menager[16], Antoine Mercier[2], Aurélien Mordret[1], Elif Oral[2], Anne Paul[1], Fabrice Peix[2], Catherine Pequegnat[1], Michel Pernoud[8], Claudio Satriano[6], Rihab Sassi[3], Marc Schaming[13], Valérie Sellier[10], Christophe Sira[15], Anne Socquet[1], Christian Sue[17,1], Aurélie Trilla[16] , Martin Vallée[6], Martijn van den Ende[2], Philippe Vernant[5], Benjamin Vial[1], Huihui Weng[2]

[1] Univ. Grenoble Alpes, Univ. Savoie Mont Blanc, CNRS, IRD, IFSTTAR, Univ. Gustave Eiffel, ISTerre, 38000 Grenoble, France, corresponding author: cecile.cornou@univ-grenoble-alpes.fr
[2] Université Côte d'Azur, IRD, CNRS, Observatoire de la Côte d'Azur, Géoazur, Valbonne, France
[3] IRSN/PSE-ENV/SCAN/BERSSIN, Fontenay-aux-roses, France
[4] BRGM, Orléans, France
[5] Géosciences Montpellier, Univ. Montpellier, CNRS, Montpellier, France
[6] Université de Paris, Institut de physique du globe de Paris, CNRS, Paris, France
[7] Laboratoire de Géologie, École Normale Supérieure, CNRS, Paris, France
[8] CEREMA Méditerranée, Valbonne, France
[9] Univ Lyon, Univ Lyon 1, ENSL, CNRS, LGL-TPE
[10] EDF-CEIDRE-TEGG, Aix-en-Provence, France
[11] Terradue Srl, Roma, Italy
[12] Laboratoire de Géologie, Université Claude Bernard Lyon 1, Villeurbanne, France
[13] IPGS, UMR7516, Université de Strasbourg/EOST, CNRS, Strasbourg, France
[14] Univ. Grenoble Alpes, CNRS, PACTE, Grenoble, France
[15] EOST; UMS830, Université de Strasbourg/EOST, CNRS, Strasbourg, France
[16] CEA, DAM, DIF, Arpajon, France
[17] CNRS UMR6249, Université Bourgogne Franche-Comté, Besançon, France

Abstract

On November 11, 2019, a Mw 4.9 earthquake hit the region close to Montelimar (lower Rhône Valley, France), on the eastern margin of the Massif Central close to the external part of the Alps. Occuring in a moderate seismicity area, this earthquake is remarkable for its very shallow focal depth (between 1 and 3 km), its magnitude, and the moderate to large damages it produced in several villages. InSAR interferograms indicated a shallow rupture about 4 km long reaching the surface and the reactivation of the ancient NE-SW La Rouviere normal fault in reverse faulting in agreement with the present-day E-W compressional tectonics. The peculiarity of this earthquake together with a poor coverage of the epicentral region by permanent seismological and geodetic stations triggered the mobilisation of the French post-seismic unit and the broad French scientific community from various institutions, with the deployment of geophysical instruments (seismological and geodesic stations), geological field surveys, and field evaluation of the intensity of the earthquake. Within 7 days after the mainshock, 47 seismological stations were deployed in the epicentral area to improve the Le Teil aftershocks locations relative to the French permanent seismological network (RESIF), monitor the temporal and spatial evolution of microearthquakes close to the fault plane and temporal evolution of the seismic response of 3 damaged historical buildings, and to study suspected site effects and their influence in the distribution of seismic damage. This seismological dataset, completed by data owned by different institutions, was integrated in a homogeneous archive and distributed through FDSN web services by the RESIF data center. This dataset, together with observations of surface rupture evidences, geologic, geodetic and satellite data, will help to unravel the causes and rupture mechanism of this earthquake, and contribute to account in seismic hazard assessment for earthquakes along the major regional Cévenne fault system in a context of present-day compressional tectonics.

Key-words : Le Teil Earthquake, Rhône valley, seismic sequence, post-seismic

1. Introduction

The French post-seismic unit ("cellule post-sismique") gathers, on a volunteer basis, scientists from various French research laboratories involved in seismological, geodetic and geological studies related to earthquakes. The unit aims at supporting the French scientific community interested in the study of major earthquakes and related natural processes by means of (1) informing the wide French scientific community on ongoing seismic sequences , (2) ensuring coordination of post-seismic actions to enhance their efficiency, and (3) guaranteing smooth operation in the field after the occurrence of an earthquake. In some cases, the unit also acts as the link between the French community involved in the intervention, the French geodetic and seismological mobile instruments managed by RESIF/CNRS-INSU (Réseau Sismologique et Géodésique Français / Centre National de la Recherche Scientifique - Institut National des Sciences de l'Univers) and representatives of French research national organisms, especially CNRS-INSU. If necessary the unit also identifies the instruments available in research laboratories for temporary use during the post-seismic intervention.

The unit is activated when its board receives an earthquake notification from international or national agencies and judges the event likely to be of interest for the French scientific community. It can also be activated upon request by the same community. The significance level of an earthquake that justifies the mobilisation of the unit depends on the context. For example, an earthquake of magnitude 5 will be considered as major if it occurs in France (metropolitan or overseas), but not if it occurs in active tectonic region along a subduction zone elsewhere on the earth. A web page is then created immediately to serve as an open centralized virtual clearinghouse that can be easily consulted with the shortest possible reaction time. Information posted on this centralized platform does not constitute a press release from the unit or the French scientific community. Content may appear, disappear, or be updated in the days following the onset of the seismic sequence. During the earthquake sequence, the unit assists in the collection and evaluation of information, the organisation of actions, the dissemination of information, and the monitoring of field actions to be carried out. The members of the unit are not necessarily involved in the field work itself. The unit participates in the identification of a head of mission who will be the main point of contact in the field.

The unit has been activated 29 times since its creation in 2009. It has been actively involved in post-seismic follow-up studies of the following earthquakes: the 2009 l'Aquila earthquake in Italy (Chiaraluce et al., 2010 ; Margheriti et al., 2011), the 2010 Maule earthquake in Chile (Lange et al., 2012), the 2012 Emilia's earthquakes sequence in Italy (Moretti et al., 2012), the 2014 Barcelonnette seismic swarm in the French Alps (De Barros et al., 2019), the 2014 Kefalonia earthquake sequence in western Greece (Perron et al., 2018), the 2016 earthquake sequence in Italy (Perouse et al., 2018; Villani et al., 2016), the 2016 Pedernales earthquake in Ecuador (Agurto-Detzel et al., 2019, Meltzer et al., 2019).

This paper describes the involvement of the French broad scientific community following the M_w 4.9 Le Teil earthquake of November 11, 2019 in Southern France, the various geological, seismological and geodetic interventions in the field, and the collected seismological data which is openly available to the scientific community within the RESIF infrastructure. Finally, it addresses some of the scientific perspectives opened by the very dense seismological network deployed in the near-fault area.

2. The M_w 4.9 Le Teil earthquake: rapid information on earthquake characteristics

At 10:52 UTC on Monday, November 11, 2019, an earthquake of local magnitude M5.4 (magnitude from CEA-LDG, Laboratoire de Détection et de Géophysique du Commissariat à l'Energie Atomique, the agency in charge of the official earthquake alerts in France) hit the region close to Montélimar (lower Rhône Valley, France), on the eastern margin of the Massif Central close to the external part of the Alps (Fig. 1a). The scientific community was informed by e-mail from BCSF (Bureau Central Sismologique Français) at 11:16 UTC. This earthquake caused damages in several villages, especially Le Teil and Viviers. During the day of November 11, revision of epicentral locations and focal mechanisms by various French research laboratories and organisms (Geoazur/OCA, SISMALP, ReNass, CEA-LDG, CSEM) provided an epicenter ranging between latitude 44.53 and 44.61 and longitude 4.61 and 4.65, i.e. west of Le Teil, and a reverse focal mechanism (Fig. 1b). Broadband waveform inversions performed by using various methods (MECAVEL : Grandin et al., 2016 ;

FMNEAR : Delouis et al., 2014 ; GRiD MT: Guilhem et al., 2013) consistently converged to a very shallow focal depth, ranging between 1 and 3.3 km depth, a mostly reverse mechanism with nodal planes trending NE-SW, and a moment magnitude Mw 4.9.

The first post-earthquake Synthetic Aperture Radar (SAR) image was acquired by the Sentinel-1 satellite (Copernicus program of the European Union, operated by the European Space Agency) on November 12, 2019, at 05:43 UTC, i.e. ~19 hours after the mainshock. Once combined with a pre-earthquake image acquired on November 6, 2019, several groups applied the Interferometric SAR (InSAR) technique to map the co-seismic surface deformation field induced by the earthquake : (1) the BRGM group used the GAMMA software on the European Space Agency (ESA) Grid Processing On Demand (GPOD) (de Michele et al., 2013), (2) the IPGP group and the Geoazur group used the NSBAS software (Grandin et al., 2017), while (3) others used the DIAPASON and SNAP softwares. These rapid analyses showed that the displacement field of the earthquake in the line-of-sight (LOS) direction of the satellite, between those two dates, was characterized by up to 5 cm displacement away and towards the satellite (Fig. 2). The unwrapped interferograms clearly indicated a shallow rupture about 4 km long reaching the surface, in the NE-SW direction, with an uplift of the SE compartment and subsidence of the NW one, in close agreement with the NE-SW trending and SE dipping nodal plane of the reverse faulting focal mechanism. Additional images were acquired with different viewing geometries on November 12 (17:39 UTC), November 16 and November 17, 2019, providing a confirmation of the occurrence of a surface rupture. On November 15, 2019, a preliminary static slip inversion including InSAR acquired both in ascending and descending geometries showed that slip was confined to a depth range shallower than ~1.5 km, with a peak slip of ~40 cm (Fig. 2). From this static inversion, the seismic moment was constrained to M0 = 2.7E16 Nm (using a shear modulus of 30 GPa), corresponding to a moment magnitude of Mw = 4.9. This preliminary inversion was performed with the assumption of uniform elastic half-space (Okada, 1985), which may not be fully valid to reproduce the second-order details of the strain field induced by earthquake slip in the shallow crust. Nevertheless, in spite of this approximation, the first-order features of the earthquake are captured by the inversion, in particular the fact that no slip at depth greater than 2–3 km is required to explain the InSAR signal.

From a geological point of view, the epicentral region has been affected by at least four main phases of deformation since the Triassic, producing a compound imprint of faulting and folding. NE-SW Mesozoic and Oligocene normal faults have been imaged in the frame of the "Géologie profonde de la France" (GPF) project, by a deep drilling in Ballazuc 27 km west of Le Teil and along a NW-SE geophysical profile combining seismic reflection and gravimetry (Bonijoly D., 1996 ; Roure et al., 1994). The Oligocene NE-SW normal faults belong to the Cévenne fault system that straddles the SE Massif Central for nearly 150 km. Folds parallel to the faults and affecting the Oligocene sediments suggest that the normal faults have been reactivated as reverse faults during the alpine orogeny (Elmi et al., 1996) (Fig. 3). Neogene to present-day NW-SE shortening in the area seen both field analysis (Blès and Gros, 1991), from GPS measurements (e.g. Masson et al., 2019) and a breakhole measurements at Boussenac 36 km north of La Rouvière (World Stress database, 2016 – wsm 00609 site FR14 ; Heidbach et al., 2018) imply that such compressive tectonics setting is still active. According to the InSAR interferograms and the very first hypocentral locations, the French geological community hypothesizes on November 13, 2019 that rupture localises on the La Rouvière fault (Fig. 3a). The 8 km long La Rouvière fault is located between, and parallel to, the St Remèze fault to the NW and the Marsanne fault to the SE (Fig. 3a). These two faults are included in the Potentially Active Faults Data Base (BDFA ; Jomard et al., 2017). The InSAR interferogram indicates uplift of the SE block and subsidence of the NW one, i.e. a SE dipping reverse fault (Fig. 2). Such geometry is compatible both with the dip of La Rouvière fault (Fig. 3b) and with the SE dipping nodal planes. However a rupture on the La Rouvière fault is not compatible with the early epicentral locations from November 11, 2019, all situated 800 to 6000 m to the NW of the InSAR surface rupture (Fig. 3a), consistent either with rupturing on another fault or a NW dipping fault plane or to a bias in earthquake location caused by a scarse coverage by permanent velocimetric and accelerometric networks (Fig. 1a). Geological field investigations conducted two days after the mainshock revealed the occurrence of surface ruptures along the InSAR rupture (see section 4), hence confirming the inherited NE-SW La Rouvière normal fault reactivated in reverse faulting during the Teil earthquake.

3. Deployment of seismological and geodetic stations

This Mw4.9 earthquake is a contemporary rare event in Southern France, an area of moderate seismicity, in terms of damage produced in several villages, especially Le Teil and Viviers, and above all because it produced surface rupture. However, similar size and shallow depth events are known to have occurred in the enlarged region in the past. Seismic swarms occurred in 1773, 1873, 1933-36 and 2002-2003 in the Tricastin region, about 20 km to the South-East of Le Teil. Significant damages were reported in nearby villages during seismic swarms in 1773 and 1873, as documented in the SisFrance database of historical earthquakes (http://www.sisfrance.net, last accessed February 4, 2020) (Fig. 1a). Thouvenot et al. (2009) found that the 2002-2003 swarm (Mmax= 1.7), located 20 km away from Le Teil event, was also very superficial (1 km depth at most).

3.1 Seismological network

The 2019 Le Teil earthquake occurred in a region poorly covered by permanent velocimetric and accelerometric networks (Fig. 1a). The closest permanent seismological station, OGLP, is located at about 20 km from the earthquake epicenter. This station recorded a maximum horizontal acceleration of 6 mg, in agreement with maximum accelerations usually measured at such epicentral distances for such magnitude. Since damages were reported in several villages close to the earthquake epicenter, and a Mw4.9 event in metropolitan France is relatively rare and could offer unique research opportunities, temporary seismological stations were rapidly installed in the epicentral area. Beyond the objective of accurately monitoring aftershocks and ground motion, some stations were deployed to target (i) monitoring of the temporal and spatial evolution of possible microcracks close to the fault plane, (ii) topographical effects that are suspected from the distribution of damages in the up-hill village of Saint-Thomé, (iii) temporal evolution of the seismic response of three damaged historical buildings (Fig. 4).

The first two broadband stations were installed in the evening of November 11 by a team from Geoazur, in a public building at the north of Montélimar and in the townhall of Le Teil. The stations started collecting data at 21:00 and 22:30, respectively. Two other stations were installed the next morning at Saint-Thomé (recording started on November 12 at 10:00) and Alba-La-Romaine (11:15). During the

four days following the earthquake and with insight on the fault location gained from the InSAR interferograms, Geoazur, ISTerre, CEREMA and IRSN installed a total of 13 broadband and 8 accelerometric stations from the RESIF-RAP, Geoazur, IRSN, CEREMA and RESIF-SISMOB mobile pools. The deployment was complemented by 28 autonomous short-period sensors (Fairfield nodes) from the RESIF-SISMOB mobile pool, 16 nodes being installed on November 12 and 13, and 8 more on November 18, especially in the vicinity of La Rouvière fault (Fig. 4). An additionnal broad-band station was installed on the La Rouvière fault December 4,2019.

Within the rapid response campaign, a special care for building response monitoring was planned. Three buildings were instrumented to record their response to aftershocks and to characterize their dynamic behavior using ambient vibration recordings. Those three instrumented structures consisted of: 1) a historical building located at Saint-Thomé (Château de Beaulieu) on the eastern edge of the hill, 2) a historical masonry tower (Tour Saint Michel) of 40 m height in the town of Viviers, and 3) the manor house of the Lafarge family located in the alluvial plain of the Rhône river. The choice of these three structures was driven by rapid accessibility, building height and structural damages observed after the mainshock. For example, at Château de Beaulieu at Saint-Thomé, several cracks were opened in interior walls. The interest on the Lafarge manor lies on its location near the Rhône river appropriate to study potential seismic amplification effects due to the alluvial plain.

Three stations (2 colocated broadband and accelerometric sensors and 1 accelerometric sensor) were telemetred to monitor aftershocks in real-time. Continuous waveforms from broadband seismological stations already operated in telemetric mode within the framework of the AlpArray project (Alparray Seismic Network, 2015; http://dx.doi.org/10.12686/alparray/z3_2015) were also freely opened to French research laboratories. On December 17, 2019, two additional broadband stations were telemetred.

In total, 47 seismological stations were deployed in the field from November 11 to 18, 2019. In addition, IRSN made available continuous recordings from 3 temporary broadband stations located about 20 km south of the epicentral area, which started to operate one week before the earthquake, and EDF

(Electricité de France) provided velocimetric and accelerometric data for the mainshock and the most significant aftershocks (M>2) from one station located at the nuclear power plant of Cruas located almost 15 km away from the epicenter.

Finally data from a set of 52 stations (Fig. 4) including velocimetric and accelerometric stations located in the vicinity of the epicentral area are distributed through FDSN Web Services by RESIF data portal or European EIDA (European Integrated Data Archive) portal. This set includes 8 different models of sensors and 7 models of acquisition units. This heterogeneous set is described in a homogeneous way by unique metadata files built in Seed dataless and stationXML formats thanks to community tools developed as part of the RESIF project. These metadata were completed and shared within a few hours of the information on each new stations. Metadata and data of the temporary stations that include the stations operated by IRSN and EDF are freely available to the wide community on the RESIF or EIDA data distribution portals (www.resif.fr, https://www.orfeus-eu.org/data/eida/, network code 3C ; http://dx.doi.org/10.15778/RESIF.3C2019). The first data from telemetric stations is available since November 16, 2019.

3.2 Distributed Acoustic Sensing deployment

The Geoazur team also connected, on November 18, 2019, a Distributed Acoustic Sensing (DAS) measurement system, provided by Febus Optics, to an existing 14-km-long section of the local telecom fibre optic network between Alba-la-Romaine, Saint-Thomé and Valvignières (Fig. 4). The system basically converts the fiber optic cable into 1400 seismometers (high-sampling-rate along-fiber strainmeters). This is the first time in Europe (and the second time in the world) that such type of measurement has been deployed in rapid response to an earthquake. The DAS interrogator recorded data until November 28, including an aftershock of magnitude 2 on November 23 as shown in Fig. 5.

3.3 GPS measurements

In addition, 4 GPS receivers were deployed in the epicentral area between November 15 and December 3, 2019 (Fig. 4). Before the Le Teil mainshock, the area of the earthquake was too scarcely covered by

permanent and temporay GNSS stations to have recorded significant co-seismic offsets and possibly post-seismic motions. According to the interferogram, we estimate that significant (> 2 mm) co-seismic deformation does not spread further than 10 km away from the rupture zone. Indeed, among the eight permanent stations from the RENAG (http://renag.resif.fr) and RGP (http://rgp.ign.fr) networks, located within 40-60 km from the epicenter, none of them show co-seismic displacements larger than 1-2 mm . temporary GNSS campaign station (from the Alps network, 52 sites measured since 1993, Vigny et al., 2002; Walpersdorf et al., 2018) is located at 30 km distance to the NNW of the epicenter. The closest temporary GNSS campaign station (from the Alps network, 52 sites measured since 1993, Vigny et al., 2001; Walpersdorf et al., 2018) is located at 30 km distance to the NNW of the epicenter.

To record a potential post-seismic signal or the co-seismic displacement due to a strong aftershock, four new temporary GNSS stations were installed at distances of less than 2 km from the surface rupture, one NW of the fault (on the footwall, which had slightly subsided), and three SE of the fault (on the hanging wall that was more largely uplifted). Two of them were located less than 1 km away from the surface rupture. The stations were installed by a team from ISTerre Grenoble and LGL-TPE Lyon, on November 15-16 and on December 3, 2019. The equipment are Topcon GB1000 receivers made available by ISTerre. The sites are set up on bedrock and monumented with forced antenna centring benchmarks. Initially, data acquisition was set to high frequency (1 sec) to monitor surface motions of strong aftershocks with high temporal resolution. After one week, the acquisition interval was switched to the standard measurement interval used for highly precise daily positioning (30 sec) to avoid memory limitations at these autonomous stations without data link transmission. The stations will be maintained for at least one year, to be able to distinguish any transient motions related to the earthquake sequence from the long term behaviour of these stations that might comport significant seasonal signals. These data will be made available through the RESIF-RENAG data archive.

4. Geological observations

Anticipating the fading and disappearance of potential ground surface ruptures caused by poor weather conditions and human activities, a team of geologists from Geosciences Montpellier, IRSN, Geoazur

and ISTerre arrived in the area on November 13, 2019. Inspecting roads and paths crossed by the deformation discontinuity identified by InSAR, the team documented in a few days about 20 field indications of surface ruptures distributed over a length of 4.5 km (Fig. 6). Those observations match the InSAR discontinuity and are parallel to but ~50m away to the SE of the pre-existing "La Rouvière" fault (Fig. 3). Some of the surface rupture indications were also surveyed with a terrestrial laser scanner to accurately quantify the deformation of the ground. In addition, two LiDAR (helicopter and drone) and one photogrammetry drone overflight campaigns were carried out to determine the continuity of the surface rupture, notably below the vegetation covering a large part of the fault thanks to the LiDAR surveys. Very shortly after the earthquake, surface rock samples from subsidiary faults were also collected by a Geoazur team to study their frictional and mechanical properties through laboratory tests and microstructural analysis. This will help to constrain future modeling of fault rupture.

5. Earthquake intensity and damages

The BCSF-ReNaSS (Bureau Central Sismologique Français – Réseau National de Surveillance Sismique) manages the collection of seismological data for earthquakes in mainland France of local magnitude greater than 3.7 (CEA-LDG) and conducts their interpretation in terms of macro-seismic intensities (severity of ground shaking) on EMS98 scale, European Macroseismic Scale (Grünthal, 1998). In case of damage, the GIM (Groupe d'Intervention Macrosismique, Macroseismic Response Group), coordinated by the BCSF-RéNaSS, establishes EMS98 intensities within a short time after the occurrence of the earthquake. This group brings together scientists (researchers, engineers) from various French laboratories involved in earthquake studies (tectonics, geology, civil engineering, etc.). Since 2007, the GIM has been activated 6 times.

Unlike the magnitude, which is calculated from seismological records, the macroseismicity is only known by analysing the observable effects on people, objects and structures in each location. For the Le Teil earthquake, more than 2000 people who felt the tremor responded to the online survey via the www.franceseisme.fr website, allowing a preliminary and rapid estimate of the earthquake intensity. On November 12, 2019, the BCSF-RéNaSS launched a survey toward the municipal authorities using

a form designed for the townhalls of the municipalities potentially affected. Given the damage described in the survey, the GIM was activated to accurately assess the EMS98 intensities of municipalities near the epicentre based on the damages observed on buildings and taking into account their vulnerability.

Among the almost sixty experts that compose the GIM, seven experts from IRSN, ISTerre/RESIF-RAP, CEREMA, PACTE, IPGS and EOST/BCSF-RéNaSS engaged in this task. Divided into teams of 2 or 3, they inspected 24 municipalities between November 18 and 22, 2019. They were assisted by mayors or municipal services, and sometimes accompanied by the fire brigade as in the case of the Le Teil municipality. More than a hundred buildings of different vulnerability levels were inspected. In the majority of cases, they were damaged by cracks, sometimes significant, open and numerous. Few of the oldest buildings built mostly in the 19th century, associated with vulnerability class A, partially or totally collapsed in the most affected areas such as Le Teil and Viviers. Among buildings of similar vulnerability, damages are more important on top of hills (Saint-Thomé) and on sedimentary filling (Savasse), attesting local site effects. The highest intensities reach locally VIII in La Rouvière and Mélas, two neighbourhoods of Le Teil that are located the closest to the northern tip of the La Rouvière fault. These are the highest intensities observed in mainland France since the 1967 Mw5.1 Arette earthquake in the Pyrenees (Cara et al., 2008 ; Rothé, 1972).

The macroseismic intensities EMS98, estimated during the GIM's field missions, are one of the major inputs for decision-making by the official French commission that classifies municipalities in a state of natural disaster. That decision triggers insurance coverage of damages. In the case of Le Teil, the GIM analysed 9 of the most affected municipalities on November 18 and 19, 2019, and provided a report for the accelerated commission that met on November 20. All of these 9 municipalities were classified in a state of natural disaster. During the commission meeting of December 11, 2019, 10 more out of the 15 others studied by the GIM were classified as such.

6. Scientific potential of the collected seismological data three months after the earthquake

Due to the low seismicity after the mainshock, most of the temporary seismological stations have been dismantled between January 14 and February 7, 2020. Only 3 broadband stations (STIL, CLAU, THOM) and 1 accelerometer (XX01 colocated with THOM) were still in place at the end of February 2020 (see www.resif.fr, network code 3C for the exact location). We present in this section some scientific perspectives related to the seismological data recorded by the very dense network deployed after the mainshock, and operated for 3 months.

6.1 Le Teil aftershocks sequence

Any analysis of aftershock patterns must rely on a robust seismicity catalog for which the threshold value for magnitude completeness (Mc) over time and space is well controlled. One priority in the design and evolution of the temporary network (Fig. 4) was to improve the Le Teil aftershock locations relatively to the regional permanent seismic network (Fig. 1a). Indeed, most of the epicentral locations of the mainshock provided by various seismological centers November 11, 2019, are shifted towards the NW compared to the observed surface faulting La Rouvière fault (Fig. 3), most probably caused by a poor coverage of permanent seismological stations (Fig 1a) and a velocity model not specific for this region (see next section). The epicenter location biases for the mainshock as introduced by the spatial paucity of permanent stations in the region is evidenced when SISMALP relocated the mainshock by adding first arrivals from seismic waveforms recorded by Alparray and IRSN temporary stations and permanent EDF station (Fig. 4). The mainshock is shifted 6 km eastward, within one km from the surface rupture (Fig. 8a).

The magnitude of completeness for the recorded seismicity varies through time according to the evolution of the temporary networks. For the sake of consistency (robustness of event counting over time), our preliminary analysis only uses seismic events (i) located within the 3 months following the mainshock (ii) with location and magnitude scale from a single data center, SISMALP, (iii) with

location determined by merging the regional data from the permanent network and the real-time temporary seismic stations and (iv) using the regional velocity model of Thouvenot et al. (2003).

The permanent SISMALP center located 30 aftershocks from November 11, 2019 to February 11, 2020. Among these, only 12 events had M>=1 (Fig. 8c). This number remains three times lower than that of previous mainshocks of similar magnitude in mainland France: about 35 aftershocks for the 1996 Ml=5.2 Saint-Paul-de-Fenouillet (Pyrénnées) and Ml=4.9 Epagny (Alps) earthquakes (Fréchet et al. 1999) considering the same time scale (3 months) and aftershock magnitude threshold (M>1). The available data support a low but steady activity, exceeding the pre-mainshock seismicity rate, that lasts for at least three months after the mainshock (Fig. 8c). The relative deficit of Le Teil aftershock rate is controlled by the weak productivity early on. Nevertheless, at a global scale the aftershock productivity for a given mainshock magnitude is known to have large variability; a 3-fold aftershock productivity variation is not rare (Dascher-Cousineau et al., 2020).

Considering M>=1 events only, the spatial pattern of the aftershocks (Fig. 8a) indicates a clustering of events within 1-fault length distance from the co-seismic faulting, as expected from worldwide patterns (e.g. Parsons and Velasco 2009, Tahir et al. 2012, Tahir and Grasso, 2015, De Arcangelis et al. 2016, Dascher-Cousineau, et al. 2020). Most of these events are in the hanging wall as common in thrust faulting sequences. Ongoing work, using a local velocity model and all the seismic stations including extraction of very small magnitude events through template matching (e.g. De Barros et al., 2019), will refine the hypocenter locations to resolve detailed 3D patterns of seismic failure. A first insight of possible improvements on the aftershock spatial distribution is exemplified by epicenter relocations that use data from all dense networks that were deployed (Fig. 8b): the cluster of aftershocks, considering magnitudes from -1.0 to 3.0, is less diffuse than suggested by the original locations (Fig. 8a). Furthermore, the aftershocks localize within the hanging wall, closer to the fault trace than the initial locations (Fig. 8a,b).

6.2 A peculiar velocity structure in the epicenter area

Two weeks after the M_w4.9 earthquake, a first shear-wave velocity model representative of the epicentral region was produced. This velocity model was inferred from the analysis of 5 days of continuous seismic ambient noise recorded synchronously by 4 telemetred broad band stations (Fig. 9a). Dispersion curves were extracted by using the 3-component RTBF algorithm (Wathelet et al., 2018) implemented in the Geopsy software (Wathelet et al., 2020) which allows to extract phase velocities of Rayleigh and Love waves, as well as the signed ellipticity of Rayleigh waves. Dispersion estimates of both Rayleigh and Love waves are very clear from 0.1 Hz to 0.5 Hz (Figure 9b-c-d). The strong directionality of the seismic noise wavefield counter-balances the small number of available seismological stations (Figure 9e). Inversion of surface waves dispersion data to get the shear-wave velocity profile was performed by using the Conditional Neighborhood Algorithm (Wathelet, 2008). The ground model parameterization used in the inversion was driven by the 4.6 km deep borehole of Valvignières located 2.4 km WSW of Saint Thomé (see Banque de Données du Sous-Sol available at http://infoterre.brgm.fr, Fig. 2, Fig. 9a) and the measured wavelength range (from 3.2 km to 30.5 km) that allows – as a rule of thumb – to correctly resolve shear-wave velocities from 1 km to 10 km depth (Foti et al., 2018). Two other deep boreholes are located nearby further inside the basin (Savasse et Marsanne boreholes, Fig 9a) and show a thickening of the geological units towards East (almost 2 km depth for the tithonian base). The deep borehole of Valvignières shows alternance of marls and limestones (hauterivian, Lower Cretaceous) from the surface down to 889 m depth with a fault zone at the base, then, a competent limestone (mostly tithonian and kimmeridgian from Upper Jurassic age) from 889 m to 1165 m depth, and claystones (from Lower to Upper Jurassic age, called “Terres Noires”) down to the sandstones of Triassic age at 4100 m depth. A simple increasing seismic velocity with depth that mimics the Sismalp velocity model (Thouvenot et al., 2003) did not lead to satisfactory fit of the measured Rayleigh and Love dispersion curves. We thus introduced in the ground model parameterization a possible low velocity zone related to the claystone formation at depths larger than 1000 m. Inverted compressional (*Vp*) and shear (*Vs*) profiles are displayed in Figure 10f and 10g, respectively. While the first upper 1200 m exhibit large *Vs* values (*Vs* probably up to 3.5 km/s in the

Tithonic limestone), shear-wave velocities at larger depth (> 1.2 km depth) are found as low as 1.4 km/s over a layer of 1 km thickness, most probably in the upper claystone formation. Such low *Vs* value at large depth has also been observed in a claystones formation in Tournemire (France) by Zillmer et al. (2014) and in the eastern part of the Paris basin (Mari and Yven, 2019). Those claystone formations are also caracterized by high Vp/Vs ratios, close to 2. The depth of the triassic bedrock, expected at about 4 km depth according to the Valvignières borehole, is not resolved by the inversion, nor is the fine velocity layering within the first kilometer.

The inverted velocity profile supports a seismic rupture occuring in the most brittle part of the shallow crust as witnessed by InSAR interferograms (Fig. 2) and the mainschok hypocenter depth (see section 2). As outlined in Roure et al. (1994) and shown by the geological cross-sections in Fig. 3 and two other deep boreholes located nearby further inside the basin (in towns of Savasse and Marsanne, Fig. 9a), the epicentral region is located at the border of the Rhône Valley which exhibits large lateral variation of geological facies and thickness. 3D seismic tomography including all seismological passive and active data recorded within the 3 months of the post-seismic experiment, together with the account for possible significant velocity anisotropy and large *Vp/Vs* ratios in the thick claystone unit (Zillmer et al., 2014), should help determine a local 3D velocity model. This model is mandatory to obtain accurate aftershocks relocations, to refine the inversion for the mainshock rupture mechanism and to simulate the strong ground motion.

6.3 Ground motion

Although the number of aftershocks recorded within 3 months after the earthquake is small, their recording by a very dense network of stations opens perspectives for the understanding of aftershock mechanics, the spatial variation of the near-fault seismic ground motion and local site effects. As an illustration, Peak Ground Velocities (PGVs) recorded during the November 23, 2019, M2 aftershock (Fig. 10a) highlight rapid decrease of ground motion amplitude beyond 3 km from the epicenter and a large spatial variability of ground motion (up to a factor of 10 between 2 and 5 km from the epicenter) (Fig. 10b). Seismograms recorded for this aftershock also outline an increase of ground motion duration

on all components for the closest stations located north of the epicenter (see recordings at stations XX03 and TEIL for the north component in Fig. 10c), possibly related to the rupture process or to the presence of a less compact/fractured geological formation. Interestingly also, large PGV on the two horizontal components were recorded 10 km apart from the epicenter (station N27, Figure 10a) at the Lafarge manor, which suffered seismic damages during the mainshock. The large PGV suggests these damages were related to amplification effects due to the alluvial plain. Finally, Fig. 11 shows velocities (north component) recorded at different levels of the Saint Michel historical masonry tower. The larger recorded motion occurred at specific frequencies at the top of the tower (Fig 11). Such seismic records will contribute to understand the seismic response of the tower, to understand observed damages and to monitor the evolution of its structural health since the mainshock.

Conclusion

The 2019 Le Teil earthquake has largely mobilised the broad French scientific community from various laboratories and institutions. The rapid response activities spanned from the deployment of instruments (seismological and geodetic stations) and field observations (geology) to the evaluation of the intensity of the earthquake. The French post-seismic unit has largely contributed to coordinate the efforts of the several geology, seismology and geodesy groups deployed in the field and the laboratory groups dedicated to refining mainshock relocation and magnitude estimation and on analysing satellite data. In particular, the early availability of InSAR interferograms to the community through the open centralized information platform managed by the French post-seismic unit was the key input to drive the deployment of seismological stations as close as possible to the ruptured fault and for the search for ground surface ruptures along the fault. Thanks to the RESIF national structuration, all the seismological data collected by the different institutes are being integrated in a homogeneous archive available to the community.

This paper gives a first glimpse on the scientific perspectives offered by the seismological data acquired by the very dense network installed after the mainshock. Data sets collected by the different

communities (surface rupture observations, LIDAR survey along the fault trace, InSAR interferograms, inventory of building damages, fiber optic survey, geodetic and seismological data) are extremely rich and complementary. They open routes to several research projects, including refinement of the active fault database and deep borehole drilling in the epicentral area, relocation of the mainshock, analysis of rupture mechanisms during the mainshock and nucleation process (Mordret et al., 2020), assessment of potential relation to anthropogenic activity, calibration and simulation of the maximum ground accelerations during the mainshock (Causse et al., 2020), evaluation of the recurrence of similar earthquakes on the fault (or, conversely, singularity of this earthquake over the last 10,000 years), impact of the current compressive tectonics on the reactivation of the Cévenne fault system branches, impact of surface rupturing on seismic hazard (Ritz et al., 2020).

Acronyms

BCSF : Bureau Central de Sismologique Français

BRGM: Bureau de Recherches Géologiques et Minières

CEA : Commissiarat à l'Energie Atomique

CEREMA : centre d'études et d'expertise sur les risques, l'environnement, la mobilité et l'aménagement

CNRS : Centre National de la Recherche Scientifique

CSEM : Centre Sismologique Euro-Méditerrannéen

EDF : Electricité de France

EOST : Ecole et Observatoire des Sciences de la Terre

INSU : Institut National des Sciences de l'Univers

IPGP : Institut de Physique du Globe de Paris

IPGS : Institut de Physique du Globe de Strasbourg

IRSN : Institut de Radio-Protection et de Sûreté Nucléaire

ISTerre: Institut des Sciences de la Terre

LDG : Laboratoire de Détection Géophysique

LGL-TPE : Laboratoire de Géologie de Lyon, Terre, Planètes, Environnement

OCA: Observatoire de la Côte d'Azur

OSUG : Observatoire des Sciences de l'Univers de Grenoble

PACTE : Laboratoire de Sciences Sociales

RAP : Réseau Accélérométrique Permanent

RéNass : Réseau National de Surveillance Sismique

RESIF: Réseau Sismologique et Géodésique Français

Acknowledgments

We acknowledge mayors and inhabitants of le Teil, Viviers, Aubinas, Saint Thomé, Alba-la-Romaine, Larnas and Chateauneuf-du-Rhône who help us in deployment of seismological and geodetic stations in the field. We acknowledge prefectures and SIDPC of Drôme and Ardèche departments, and mayors, town hall employers and inhabitants of the 24 cities visted by the GIM Team. Field experiments were supported by fundings from ISTerre, Géoazur, CEREMA, IRSN, Géosciences Montpellier, LGL-TPE, PACTE, EOST/BCSF-RéNass, RAP-RESIF, INSU, Action Transversale Sismicité (ATS) of RESIF. RESIF is a national Research Infrastructure recognized as such by the French Ministry of higher education and research. It is additionally supported by a public grant overseen by the French national research agency (ANR) as part of the "Investissements d'Avenir" program (reference: ANR-11-EQPX-0040) and the French Ministry of ecology, sustainable development and energy. RESIF; (1995): RESIF-RLBP French Broad-band network, RESIF-RAP strong motion network and other seismic stations in metropolitan France; RESIF - Réseau Sismologique et géodésique Français. http://dx.doi.org/10.15778/RESIF.FR. RESIF; (1995): RESIF-RAP French Accelerometric Network; RESIF - Réseau Sismologique et géodésique Français.http://dx.doi.org/10.15778/RESIF.RA. Bertrand, E., Cornou, C., Gélis, C., Rivet, D., & SISMOB-RESIF. (2019). Le Teil P5 post seismic experiment. RESIF - Réseau Sismologique et géodésique Français. https://doi.org/10.15778/10.15778/RESIF.3C2019. AlpArray Seismic Network; (2015): AlpArray

Seismic Network (AASN) temporary component. AlpArray Working Group. http://dx.doi.org/10.12686/alparray/z3_2015.

Sentinel-1 data used in this study is copyright of European Commission (EU), Copernicus program, operated by the European Space Agency (ESA). The data was obtained via the PEPS portal of the Centre National d'Etudes Spatiales (CNES). The DAS measurements were made on the Ardèche Drôme Numérique telecom network with the help of the people from the ADTIM company in charge of the network. Information on the historical earthquake were extracted from the SisFrance, BRGM, EDF, ISRN database (last accessed, February 4, 2020).

References

Agurto-Detzel, H., Font, Y., Charvis, P., Régnier, M., Rietbrock, A., Ambrois, D., Paulatto, M., Alvarado, A., Beck, S., Courboulex, F., de Barros, L., Deschamps, A., Hernandez Salazar, M.-J., Hernandez, S., Hoskins, M., Leon-Rios, S., Lynner, C., Meltzer, A., Mercerat, D., Michaud, F., Nocquet, J.-M., Rolandone, F., Ruiz, M., Soto-Cordero, L., 2019. Ridge subduction and afterslip control aftershock distribution of the 2016 Mw 7.8 Ecuador earthquake, Earth and Planetary Science Letters, 520, 63-76.

AlpArray Seismic Network, 2015. AlpArray Seismic Network (AASN) temporary component. AlpArray Working Group. http://dx.doi.org/10.12686/alparray/z3_2015

Blès, J.L., Gros, Y., 1991. Stress field changes in the Rhone Valley from the Miocene to the present. Tectonophysics, 194, 265-277.

Bonijoly, D., Perrin, J., Roure, F., Bergerat, F., Courel, L., Elmi, S., GPF team, Mignot, A., 1996. The Ardèche palaeomargin of the South-East Basin of France: Mesozoic evolution of a part of the Tethyan continental margin (Géologie Profonde de la France programme), Marine and Petroleum Geology, 13, 6, 607-623.

Cara M., Alasset PJ., Sira C., 2008. Magnitude of Historical Earthquakes, from Macroseismic Data to Seismic Waveform Modelling: Application to the Pyrenees and a 1905 Earthquake in the Alps. In: Fréchet J., Meghraoui M., Stucchi M. (eds) Historical Seismology. Modern Approaches in Solid Earth Sciences, vol 2. Springer, Dordrecht, pp. 363-378.

Chiaraluce, L., Chiarabba, C., De Gori, P., Di Stefano, R., Improta, L., Piccinini, D., Schlagenhauf A., Traversa P., Valoroso L & Voisin, C., 2011. The 2009 L'Aquila (Central Italy) Seismic Sequence. Bollettino di Geofisica Teorica e Applicata. 52 (3), 367-38.

Causse, M., Cornou, C., Maufroy, E., Grasso, R.-R., Baillet, L., El Haber, E., 2020. Exceptional ground motion for moderate-sized shallow earthquake, submitted to Nature Geoscience

Dascher-Cousineau, K., Brodsky, E. E., Lay, T., Goebel, T. H., 2020. What controls variations in aftershock productivity?, Journal of Geophysical Research: Solid Earth, 125(2), e2019JB018111.

De Arcangelis, L., Godano, C., Grasso, J. R., Lippiello, E., 2016. Statistical physics approach to earthquake occurrence and forecasting. Physics Reports, 628, 1-91.

De Barros, L., Baques, M., Godano, M., Helmstetter, A., Deschamps, A., Larroque, C., Courboulex, F., 2019. Fluid-Induced Swarms and Coseismic Stress Transfer: A Dual Process Highlighted in the Aftershock Sequence of the 7 April 2014 Earthquake (Ml 4.8, Ubaye, France). Journal of Geophysical Research: Solid Earth, 124(4), 3918-3932.

De Michele, M., Briole, P., Raucoules, D., Lemoine, A., Rigo, A., 2013. Revisiting the shallow M_w 5.1 Lorca earthquake (southeastern Spain) using C-band InSAR and elastic dislocation modelling, Rem. Sens. Lett., 4(9), 863–872.

Delouis, B., 2014. FMNEAR: Determination of focal mechanism and first estimate of rupture directivity using near-source records and a linear distribution of point sources. Bulletin of the Seismological Society of America, 104(3), 1479-1500.

Elmi S., Busnardo R., Clavel B., Camus G., Kieffer G., Bérard P. and B. Michaëly, 1996. Notice explicative, Carte géologique de France (1/50 000), Feuille Aubenas (865). Orléans : BRGM, 170 p. Carte géologique par Y. Kerrien (coord.), S. Elmi, R. Busnardo, G. Camus, G. Kieffer, J. Moinereau, A. Weisbrod (1989).

Foti, S., Hollender, F., Garofalo, F., Albarello, D., Asten, M., Bard, P. Y., Comina, C., Cornou, C., Cox, B., Di Giulio, G., Forbriger, T., Hayashi, K., Lenedei, E., Martin, A., Mercerat, D., Ohrnberger, M., Poggi, V., Renalier, F., Sicilia, D., Socco, V., 2018. Guidelines for the good practice of surface wave analysis: A product of the InterPACIFIC project. Bulletin of Earthquake Engineering, 16(6), 2367-2420.

Fréchet, J., Rigo, A., Souriau, A., Thouvenot, F., 1999. Comparison of two damaging earthquakes in France in 1996 : Saint-Paul-de-Fenouillet (Pyrenees) and Epagny (Alps), CNFFG, Quadriennal report 1995-1998, XXII, UIGG General Assembly, Birmingham, 59-70.

Grandin, R., Klein, E., Métois, M., Vigny, C., 2016. Three-dimensional displacement field of the 2015 Mw8. 3 Illapel earthquake (Chile) from across-and along-track Sentinel-1 TOPS interferometry. Geophysical Research Letters, 43(6), 2552-2561.

Grünthal G., 1998. European Macroseismic Scale 1998 (EMS-98), European Seismological Commission, sub commission on Engineering Seismology, Working Group Macroseismic Scales. Conseil de l'Europe, Cahiers du Centre Européen de Géodynamique et de Séismologie, Vol. 15, Luxembourg.

Guilhem A., Dreger, D. S., Kawakatsu, H., Hiroshi, H., 2013. Moment tensors for rapid characterization of megathrust earthquakes: the example of the 2011 M9 Tohoku-oki, Japan earthquake, Geophysical Journal International, 192 (2), 759-772.

Heidbach, O., Rajabi, M., Cui, X., Fuchs, K., Müller, B., Reinecker, J., Reiter K, Tingay M., Wenzel F., Xie, F., Ziegler, M. O., Zoback M.-L., Zoback M., 2018. The World Stress Map database release 2016: Crustal stress pattern across scales. Tectonophysics, 744, 484-498.

Jomard, H., Cushing, E. M., Palumbo, L., Baize, S., David, C., Chartier, T., 2017. Transposing an active fault database into a seismic hazard fault model for nuclear facilities – Part 1: Building a database of potentially active faults (BDFA) for metropolitan France, Nat. Hazards Earth Syst. Sci., 17, 1573–1584, 2017.

Lange D., Tilmann, F., Barrientos, S.E., Contreras-Reyes, E., Pascal Methe, P., Moreno, M., Heit, B., Agurto, H., Bernard, P., Vilotte, J.P., Beck, S., 2012. Aftershock seismicity of the 27 February 2010 Mw 8.8 Maule earthquake rupture zone, Earth and Planetary Science Letters, 317-318, 413-425.

Margheriti, L., Husen, S., Chiaraluce, L., Voisin, C., Cultrera, G., Govoni, Moretti, M., Bordoni, P., Luzi, L., Azzara, R., Valoroso, L., Di Stefano, R., Mariscal, A., Improta, L., Pacor, F., Milana, G., Mucciarelli, M., Parolai, S., Amato, A., Chiarabba, C., De Gori, P., Lucente, F. P., Di Bona, M., Pignone, M., Cecere, G., Criscuoli, F., Delladio, A., Lauciani, V., Mazza, S., Di Giulio, G., Cara, F., Augliera, P., Massa, M., D'Alema, E., Marzorati, S., Sobiesiak, M., Strollo, A., Duval, A.-M., Dominique, P., Delouis, B., Paul, A., Husen, S., Selvaggi, G., 2011. Rapid response seismic networks in Europe: lessons learnt from the L'Aquila earthquake emergency. Annals of Geophysics, 54 (4), 392-399.

Mari, J. L., Yven, B., 2019. Chapter 7. Integrated seismic study - Focus on “Cigéo”, the French geological repository project, in Seismic imaging: a practical approach, pp. 163-200, DOI: 10.1051/978-2-7598-2351-2.c009

Masson, C., Mazzotti, S., Vernant, P., & Doerflinger, E., 2019. Extracting small deformation beyond individual station precision from dense Global Navigation Satellite System (GNSS) networks in France and western Europe, Solid Earth, 10, 1905–1920.

Meltzer, A., Beck, S., Ruiz, M., Hoskins, M., Soto-Cordero, L., Stachnik, J. C., Lynner, C., Porritt, R., Portner, D., Alvarado, A., Hernandez, S., Yepes, H., Charvis, P., Font, Y., Regnier, M., Agurto-Detzel, H., Rietbrock, A., Leon-Rios, S., Mercerat, D., 2019. The 2016 Mw 7.8 Pedernales, Ecuador, Earthquake: Rapid Response Deployment, Seismological Research Letters, 90 (3), 1346-1354.

Mordret, A., Brenguier, F., Causse, M., Boué, P., Voisin, C., Dumont, I., Vernon, F. L., Ampuero, J.-P., 2020. Seismic Stereometry reveals preparatory behavior and source kinematics of intermediate-size earthquakes, submitted to Geophysical Research Letters

Moretti, M., Abruzzese, L., Zeid, N. A., Augliera, P., Azzara, R. A., Barnaba, C., Benedetti, L., Bono, A. Bordoni, P., Boxberger, T., Bucci, A., Cacciaguerra, S., Calò, M., Cara, F., Carannante, S., Cardinale, V., Castagnozzi, A., Cattaneo, M., Cavaliere, A., Cecere, G., Chiarabba, C., Chiaraluce, L., Ciaccio, M. G., Cogliano, R., Colasanti, G., Colasanti,M., Cornou, C., Courboulex, F., Criscuoli, F., Cultrera, G., D'Alema, E., D'Ambrosio, C., Danesi, S., De Gori, P., Delladio, A., De Luca, G., Demartin, M., Di Giulio, G., Dorbath, C., Ercolani, E., Faenza, L., Falco, L., Fiaschi, A., Ficeli, P., Fodarella, A., Franceschi, D., Franceschina, G., Frapiccini, M., Frogneux, M., Giovani, L., Govoni, A., Improta, L., Jacques, E., Ladina, C., Langlaude, P., Lauciani, V., Lolli, B., Lovati, S., Pio Lucente, F., Luzi, L., Mandiello, A., Marcocci, C., Margheriti, L., Marzorati, S., Massa, M., Mazza, S., Mercerat, D., Milana, G., Minichiello, F., Molli, G., Monachesi, G., Morelli, A., Moschillo, R., Pacor, F., Piccinini, D., Piccolini, U., Pignone, M., Pintore, S., Pondrelli, S., Priolo, E., Pucillo, S., Quintiliani, M., Riccio, G., Romanelli, M., Rovelli, A., Salimbeni, S., Sandri, L., Selvaggi, G., Serratore, A., Silvestri, M., Valoroso, L., Van der Woerd, J., Vannucci, G., Zaccarelli, L., 2012. Rapid response to the earthquake emergency of May 2012 in the Po Plain, northern Italy. Annals of Geophysics, 55 (4), 583-590.

Okada, Y., 1985. Surface deformation due to shear and tensile faults in a half-space. Bulletin of the seismological society of America, 75(4), 1135-1154.

Parsons, T., Velasco, A. A., 2009. On near-source earthquake triggering. Journal of Geophysical Research: Solid Earth, 114(B10).

Perouse, E., Benedetti, L., Fleury, J., Rizza, M., Puliti, I., Billant, J., van der Woerd , J., Feuillet, N., Jacques, E., Pace, B., 2018. Coseismic slip vectors of 24 August and 30 October 2016 earthquakes in Central Italy: Oblique slip and regional kinematic implications. Tectonics, 37 (10), 3760-3781.

Perron, V., Hollender, F., Mariscal, A., Theodoulidis, N., Andreou, C., Bard, P. Y., Cornou, C., Cottereau, R., Cushing, M. E., Frau, A., Hok, S., Konidaris, A., Langlaude, P., Laurendeau, A., Savvaidis, A., Svay, 2018. Accelerometer, velocimeter dense- array, and rotation sensor datasets from the sinaps@ postseismic survey (Cephalonia 2014–2015 aftershock sequence). Seismological Research Letters, 89 (2A), 678-687.

Ritz J-F., Baize S., Ferry M., Larroque C., Audin L., Delouis B., Mathot E., The Mw4.9 Le Teil surface-rupturing earthquake in southern France: A new insight into the question of seismic hazard assessment in stable continental regions, Communications Earth & Environnement, Nature, in revision.

Rothé J.-P., 1972. 13-08-1967, Arette. Annales de l'Institut de Physique du Globe, troisième partie, Tome IX, Université Louis Pasteur, Strasbourg 1972. IPGS, 82-89.

Roure F., Brun, J.-P., Colletta, B., Vially, R., 1994. Multiphase extensional structures, fault reactivation, and petroleum plays in the Alpine Foreland Basin of Southeastern France, In: Mascle A. (eds) Hydrocarbon and Petroleum Geology of France. Special Publication of the European Association of Petroleum Geoscientists, 4, pp 245-268, Springer, Berlin, Heidelberg.

Tahir, M., Grasso, J.-R., Amorése, D., 2012. The largest aftershock: How strong, how far away, how delayed?, Geophys. Res. Lett. 39, L04, 301.

Tahir, M., Grasso, J.-R., 2015. Faulting style controls for the space–time aftershock patterns. Bulletin of the Seismological Society of America, 105(5), 2480-2497.

Thouvenot, F., Fréchet, J., Jenatton, L., Gamond, J.F., 2003. The Belledonne Border Fault: identification of an active seismic strike-slip fault in the western Alps, Geophysical Journal International, 155 (1), 174–192.

Thouvenot, F., Jenatton, L., Gratier, J. P., 2009. 200 m deep earthquake swarm in Tricastin (lower Rhône Valley, France) accounts for noisy seismicity over past centuries. Terra Nova, 21(3), 203-210.

Vigny, C., Chéry, J., Duquesnoy, T., Jouanne, F., Ammann, J., Andizei, M., Avouac, J. P., Barlier, F., Bayer, R., Briole, P., Calais, E., Cotton, F., Duquenne, F., Feigl, K. L., Ferhat, G., Flouzat, M., Gamond, J.-F., Geiger, A., Harmel, A., Kasser, M., Laplanche, M., Le Pape, M., Martinod, J., Ménard, G., Meyer, B., Ruegg, J.-C., Scheubek, J.-M., Scotti, O., Vidal, G., 2002. GPS network monitors the western Alps' deformation over a five-year period: 1993–1998. Journal of Geodesy, 76(2), 63–76.

Villani, F., Civico, R., Pucci, S., Pizzimenti, L., Nappi, R., De Martini, P. M., the Open EMERGEO Working group, 2018. A database of the coseismic effects following the 30 October 2016 Norcia earthquake in Central Italy. Scientific data, *5*, 180049.

Walpersdorf, A., Pinget, L., Vernant, P., Sue, C., Deprez, A., RENAG team. (2018). Does long-term GPS in the Western Alps finally confirm earthquake mechanisms?. Tectonics, 37(10), 3721-3737.

Wathelet, M., 2008. An improved neighborhood algorithm: parameter conditions and dynamic scaling. Geophysical Research Letters, 35(9).

Wathelet, M., Guillier, B., Roux, P., Cornou, C., Ohrnberger, M., 2018. Rayleigh wave three-component beamforming: signed ellipticity assessment from high-resolution frequency-wavenumber processing of ambient vibration arrays. Geophysical Journal International, 215(1), 507-523.

Wathelet, M., Chatelain, J. L., Cornou, C., Giulio, G. D., Guillier, B., Ohrnberger, M., Savvaidis, A. (2020). Geopsy : A User-Friendly Open-Source Tool Set for Ambient Vibration Processing. Seismological Research Letters, 91(3), 1878-1889.

Zillmer, M., Marthelot, J. M., Gélis, C., Cabrera, J., & Druivenga, G., 2014. In situ seismic measurements in claystone at Tournemire (France). Geophysical Journal International, 199(3), 1798-1807.

List of Figures

Fig. 7. Map of the EMS98 intensities estimated by the field survey of the GIM between November 18 and 22, 2019.

Fig. 8. (a) Location of aftershocks by SISMALP from November 11, 2019, to February 11, 2020 using real-time temporary stations and permanent RESIF network stations, and the velocity model of Thouvenot et al. (2003). Two location of the Mw4.9 mainshock are provided: location obtained on November 11, 2019 (red star) and relocation obtained on December 12, 2019 (filled red star) using recordings from the temporary Alparray and IRSN stations and the permanent EDF station (Fig. 4). (b) Afterschocks located by the SISMALP network using permanent RESIF network stations and all temporary post-seismic stations. (c) Time distribution of the number of M>=1 events per period of 10 days after the mainshock onset and time distribution of magnitudes (local magnitude, Ml) using the 30 located aftershocks. The mainshock is indicated by the blue vertical line.

Fig. 9. (a) Location of the 4 temporary broad-band stations used to extract surface waves dispersion estimates and the three deep boreholes of Valvignières (#1), Savasse (#2) and Marsanne (#3); Histograms of (b) Rayleigh wave phase velocities, (c) Love wave phase velocities and (d) ellipticity angles as a function of frequency (colored dots; red color indicates largest number of estimates), extracted dispersion data (phase velocities, ellipticity angle) with their uncertainty (black dots), dispersion data (phase velocities, ellipticity angle) forward modeled from velocity profiles indicated in (f) and (g) (gray curves); (e) histograms of seismic noise wavefield azimuths as a function of frequency; ensemble of (f) *Vp* and (g) *Vs* profiles that explain the extracted dispersion data within their uncertainty bound. The velocity model of SISMALP (Thouvenot et al., 2003) is indicated by dash line.

Fig. 10. (a) Spatial distribution of Peak Ground Velocity (PGV) recorded by the three components (Z, N, E) of ground motion after the November 23, 2019, Ml2 aftershock (SISMALP location). Seismograms are band-bass filtered between 0.1 and 20 Hz. N27 station location is indicated by the arrow. (b) PGV as a function of epicentral distance. (c) Velocities recorded by the NS component of stations lying along a SW-NE section (from LARN to CRU1 stations, see (a)). Velocities are band-bass

filtered between 0.5 and 10 Hz and, for the sake of clarity, each seismogram is normalized by its peak ground value.

Fig. 11. Velocities (NS component) recorded at different levels of the Saint Michel historical tower during the Ml2 aftershock that occured November 23, 2019.

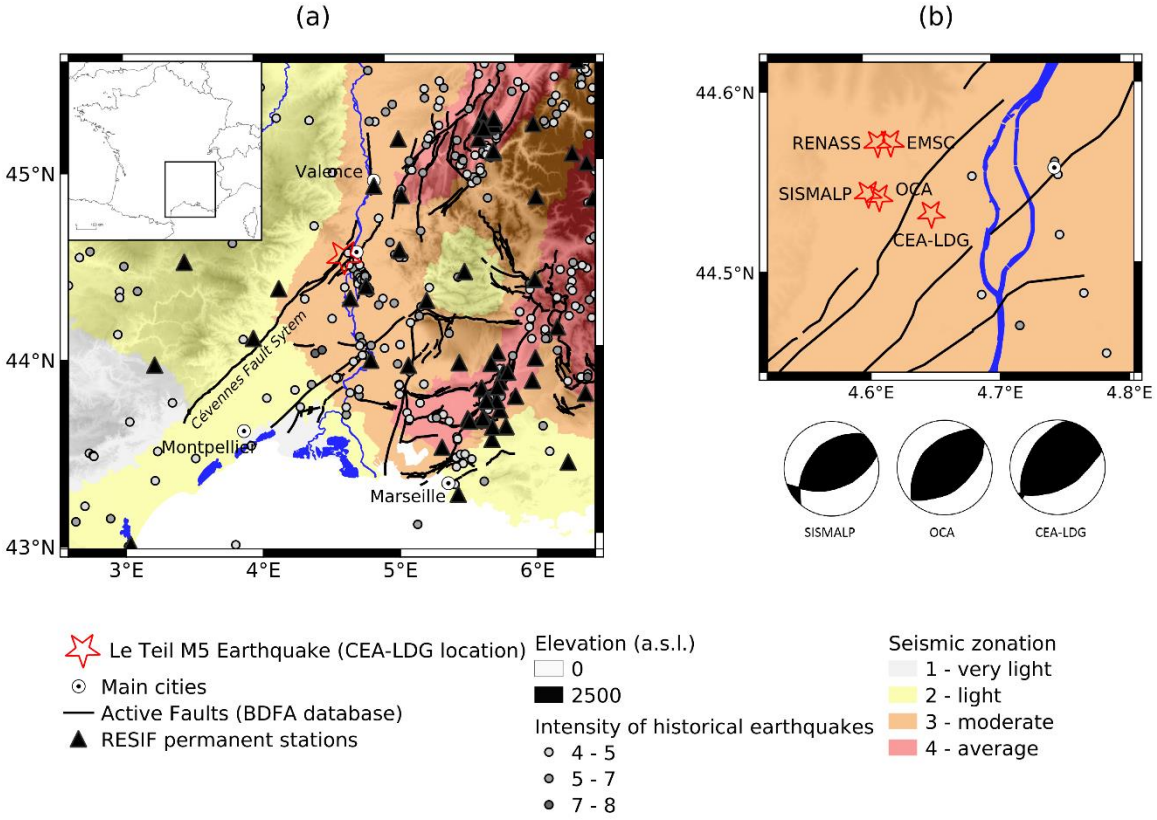
(a)
(b)
45°N
44°N
43°N
3°E
4°E
5°E
6°E
Valence
Montpellier
Marseille
Cévennes Fault System
44.6°N
44.5°N
4.6°E
4.7°E
4.8°E
RENASS
EMSC
SISMALP
OCA
CEA-LDG
SISMALP
OCA
CEA-LDG
Le Teil M5 Earthquake (CEA-LDG location)
Main cities
Active Faults (BDFA database)
RESIF permanent stations
Elevation (a.s.l.)
0
2500
Intensity of historical earthquakes
4 - 5
5 - 7
7 - 8
Seismic zonation
1 - very light
2 - light
3 - moderate
4 - average

Fig.1

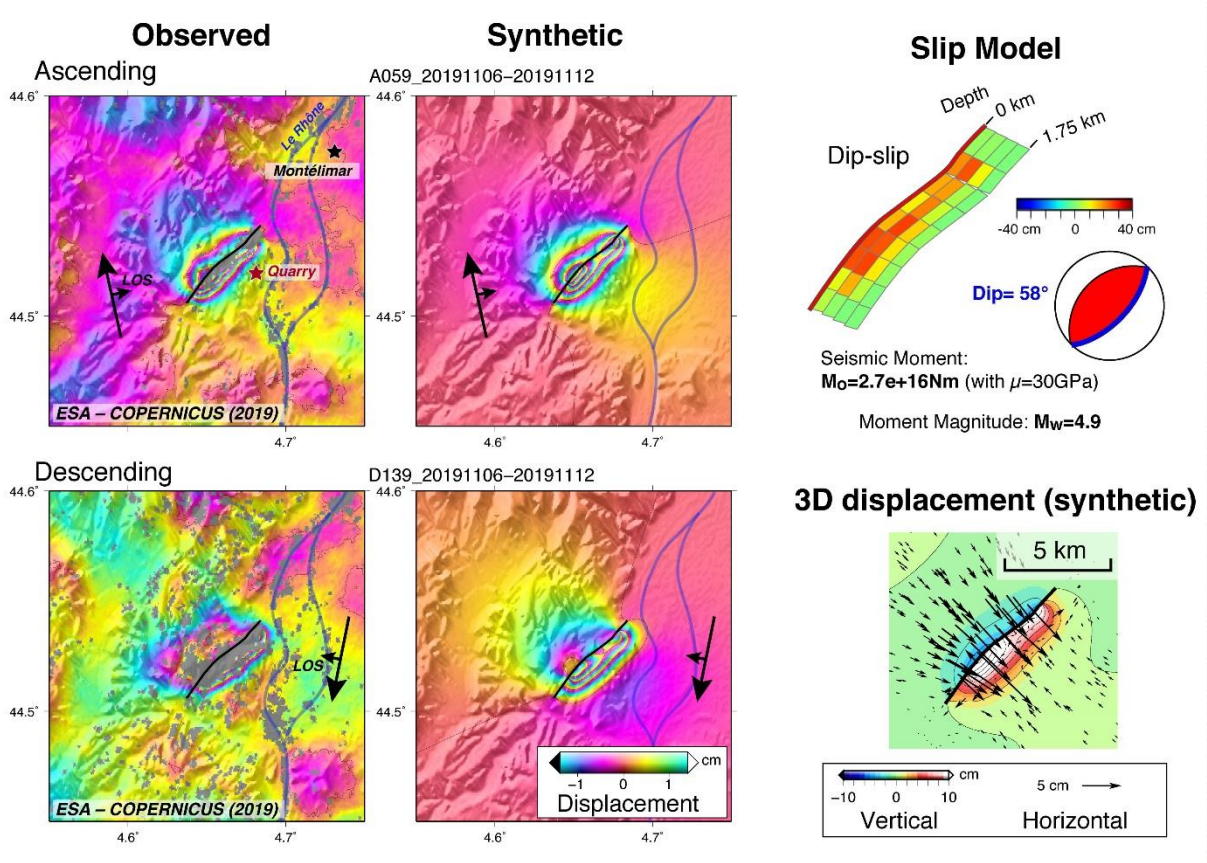
Observed
Synthetic
Ascending
A059_20191106–20191112
Le Rhône
Montélimar
Quarry
LOS
ESA – COPERNICUS (2019)
Descending
D139_20191106–20191112
LOS
ESA – COPERNICUS (2019)
cm
−1 0 1
Displacement
44.6°
44.5°
4.6°
4.7°
Slip Model
Depth
0 km
1.75 km
Dip-slip
-40 cm 0 40 cm
Dip= 58°
Seismic Moment:
M_O=2.7e+16Nm (with μ=30GPa)
Moment Magnitude: M_W=4.9
3D displacement (synthetic)
5 km
cm
−10 0 10
Vertical
5 cm
Horizontal

Fig. 2

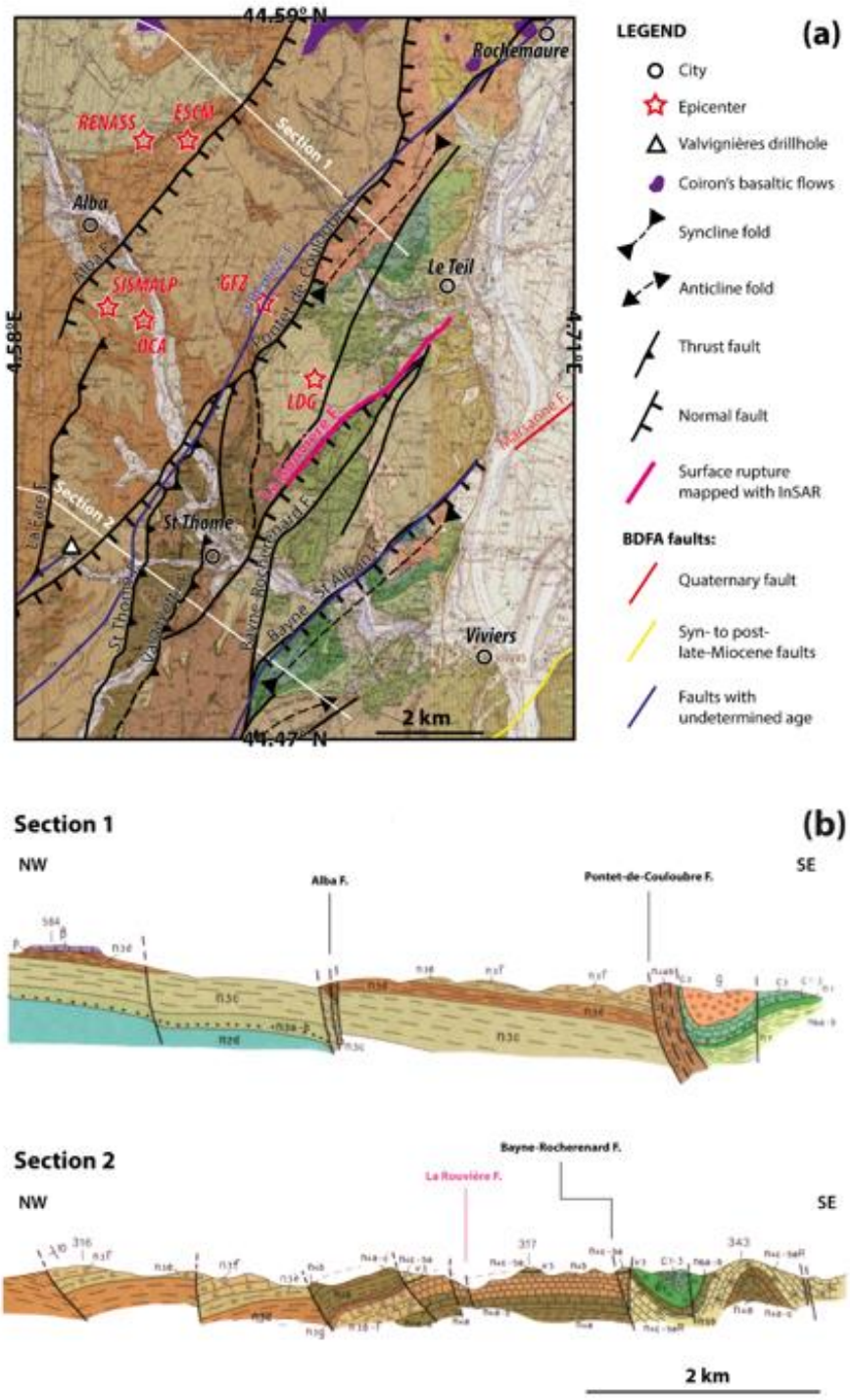
44.59° N
44.47° N
4.58° E
4.71° E
Rochemaure
RENASS
ESCM
Section 1
Alba
Alba F.
SISMALP
GFZ
OCA
Le Teil
Pontet de Couloubre F.
LDG
Bayne F.
Narcisse F.
La Faure F.
Section 2
St Thome
St Thome F.
Vaunavey F.
Bayne-Rocherenard F.
Bayne-St Alban F.
Viviers
2 km
LEGEND
(a)
City
Epicenter
Valvignières drillhole
Coiron's basaltic flows
Syncline fold
Anticline fold
Thrust fault
Normal fault
Surface rupture mapped with InSAR
BDFA faults:
Quaternary fault
Syn- to post-late-Miocene faults
Faults with undetermined age
Section 1
(b)
NW
SE
Alba F.
Pontet-de-Couloubre F.
Section 2
NW
SE
Bayne-Rocherenard F.
La Rouvière F.
2 km

Fig. 3

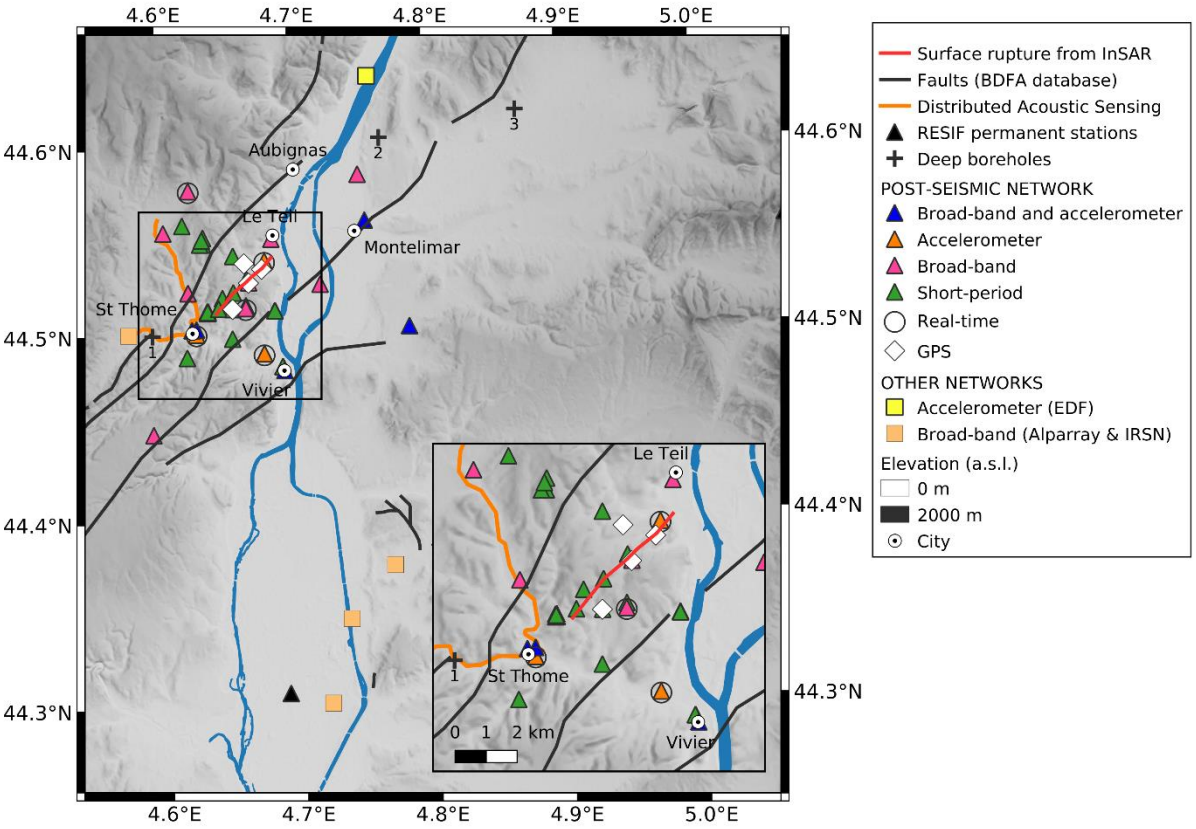
4.6°E
4.7°E
4.8°E
4.9°E
5.0°E
44.6°N
44.5°N
44.4°N
44.3°N
Aubignas
Le Teil
Montelimar
St Thome
Vivier
1
2
3
0 1 2 km
Surface rupture from InSAR
Faults (BDFA database)
Distributed Acoustic Sensing
RESIF permanent stations
Deep boreholes
POST-SEISMIC NETWORK
Broad-band and accelerometer
Accelerometer
Broad-band
Short-period
Real-time
GPS
OTHER NETWORKS
Accelerometer (EDF)
Broad-band (Alparray & IRSN)
Elevation (a.s.l.)
0 m
2000 m
City

Fig. 4

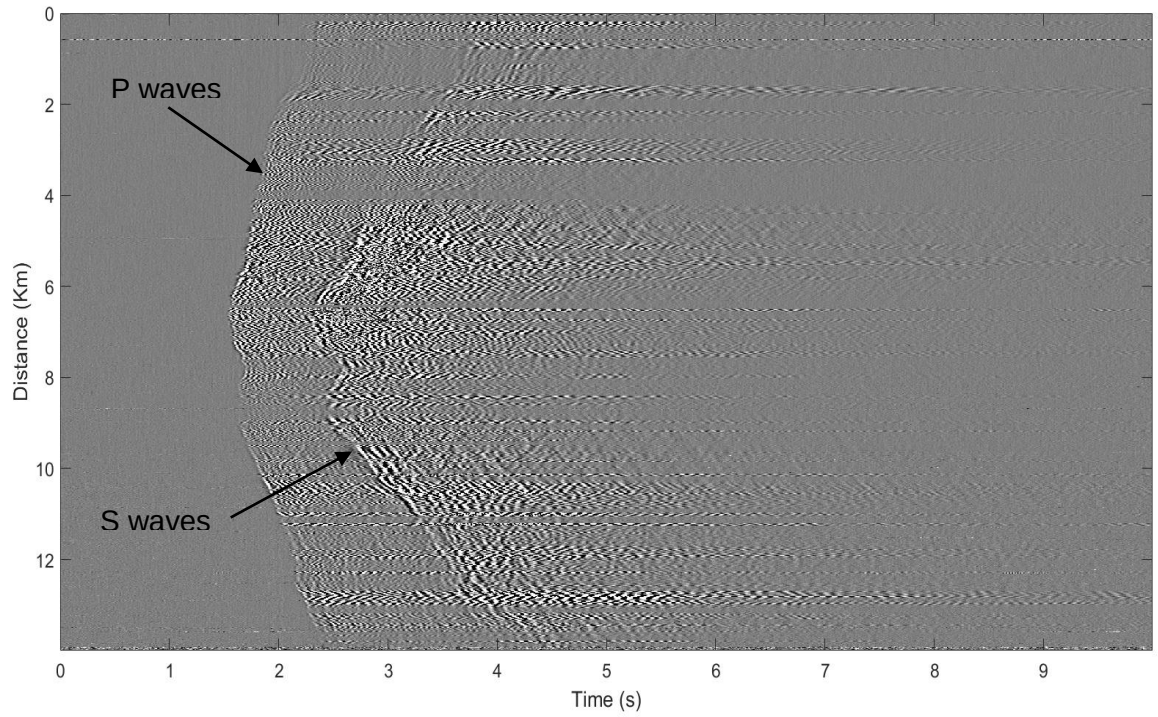

Fig. 5

Fig. 6

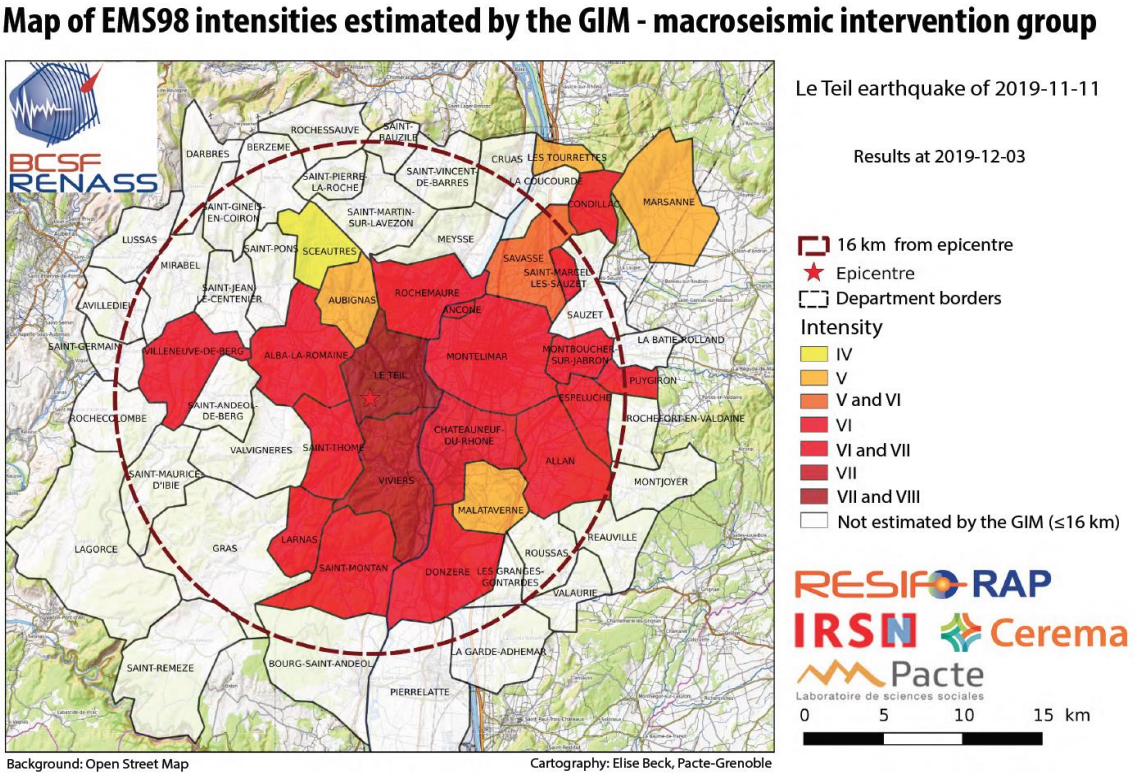
Map of EMS98 intensities estimated by the GIM - macroseismic intervention group
BCSF RENASS
Le Teil earthquake of 2019-11-11
Results at 2019-12-03
16 km from epicentre
Epicentre
Department borders
Intensity
IV
V
V and VI
VI
VI and VII
VII
VII and VIII
Not estimated by the GIM (≤16 km)
RESIF RAP
IRSN
Cerema
Pacte
Laboratoire de sciences sociales
0 5 10 15 km
Background: Open Street Map
Cartography: Elise Beck, Pacte-Grenoble
ROCHESSAUVE
SAINT-RAZILE
DARBRES
BERZEME
SAINT-PIERRE-LA-ROCHE
SAINT-VINCENT-DE-BARRES
CRUAS
LES TOURRETTES
LA COUCOURDE
CONDILLAS
MARSANNE
SAINT-GINEIS-EN-COIRON
SAINT-MARTIN-SUR-LAVEZON
LUSSAS
SAINT-PONS
SCEAUTRES
MEYSSE
SAVASSE
SAINT-MARCEL-LES-SAUZET
MIRABEL
SAINT-JEAN-LE-CENTENIER
AUBIGNAS
ROCHEMAURE
ANCONE
SAUZET
LAVILLEDIEU
SAINT-GERMAIN
VILLENEUVE-DE-BERG
ALBA-LA-ROMAINE
MONTELIMAR
MONTBOUCHER-SUR-JABRON
LA BATIE-ROLLAND
LE TEIL
PUYGIRON
ESPELUCHE
SAINT-ANDEOL-DE-BERG
ROCHECOLOMBE
ROCHEFORT-EN-VALDAINE
CHATEAUNEUF-DU-RHONE
VALVIGNERES
SAINT-THOME
ALLAN
SAINT-MAURICE-D'IBIE
VIVIERS
MONTJOYER
MALATAVERNE
LAGORCE
GRAS
LARNAS
REAUVILLE
ROUSSAS
SAINT-MONTAN
DONZERE
LES GRANGES-GONTARDES
VALAURIE
LA GARDE-ADHEMAR
SAINT-REMEZE
BOURG-SAINT-ANDEOL
PIERRELATTE

Fig. 7

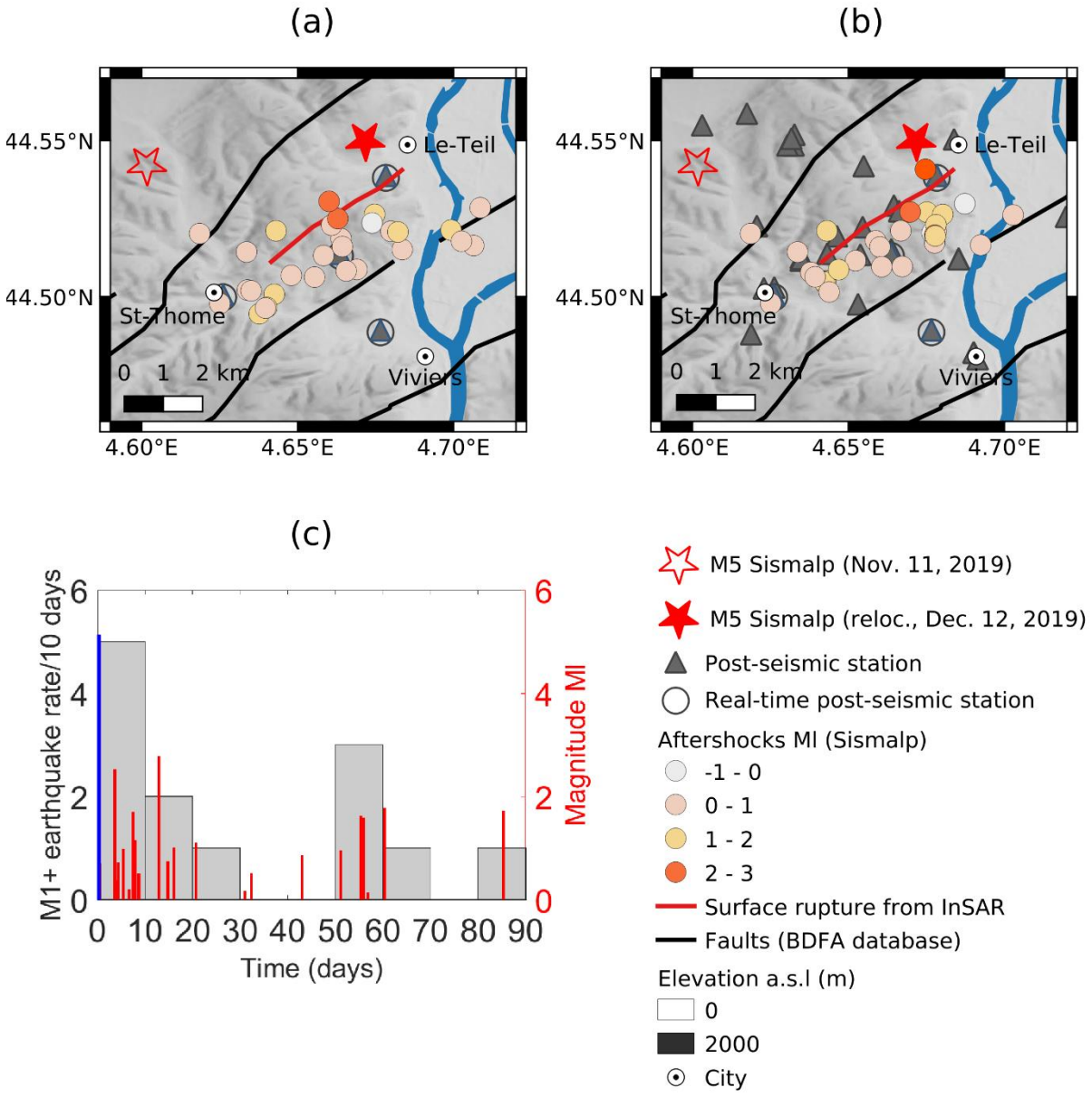
(a)
(b)
(c)
44.55°N
44.50°N
Le-Teil
St-Thome
Viviers
0 1 2 km
4.60°E
4.65°E
4.70°E
M1+ earthquake rate/10 days
Magnitude Ml
Time (days)
0 10 20 30 40 50 60 70 80 90
M5 Sismalp (Nov. 11, 2019)
M5 Sismalp (reloc., Dec. 12, 2019)
Post-seismic station
Real-time post-seismic station
Aftershocks Ml (Sismalp)
-1 - 0
0 - 1
1 - 2
2 - 3
Surface rupture from InSAR
Faults (BDFA database)
Elevation a.s.l (m)
0
2000
City

Fig. 8

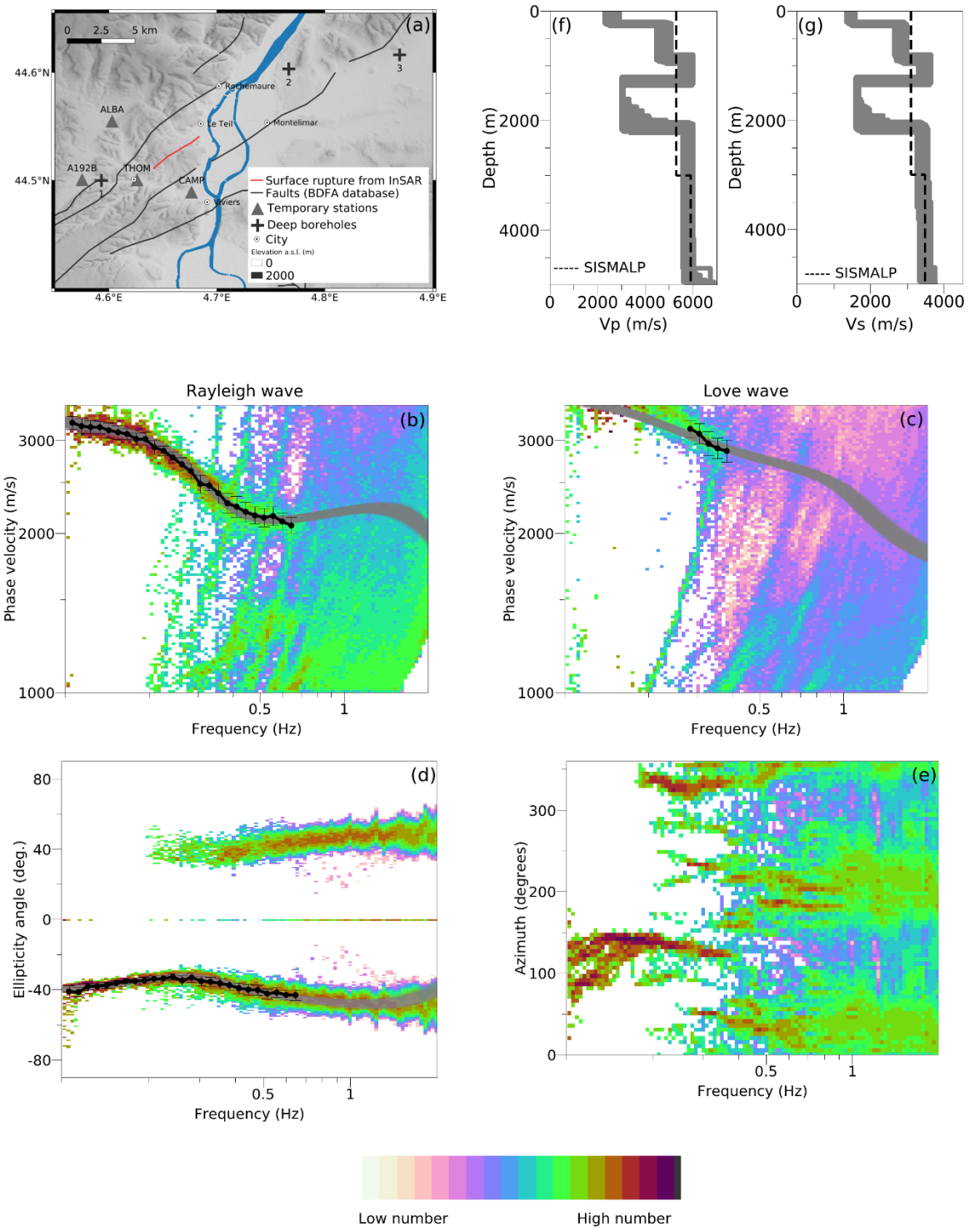
(a)
0 2.5 5 km
44.6°N
44.5°N
4.6°E
4.7°E
4.8°E
4.9°E
Rochemaure
Le Teil
Montelimar
Viviers
ALBA
A192B
THOM
CAMP
1
2
3
Surface rupture from InSAR
Faults (BDFA database)
Temporary stations
Deep boreholes
City
Elevation a.s.l. (m)
0
2000
(f)
Depth (m)
SISMALP
Vp (m/s)
(g)
Vs (m/s)
Rayleigh wave
(b)
Phase velocity (m/s)
Frequency (Hz)
Love wave
(c)
(d)
Ellipticity angle (deg.)
(e)
Azimuth (degrees)
Low number
High number

Fig. 9

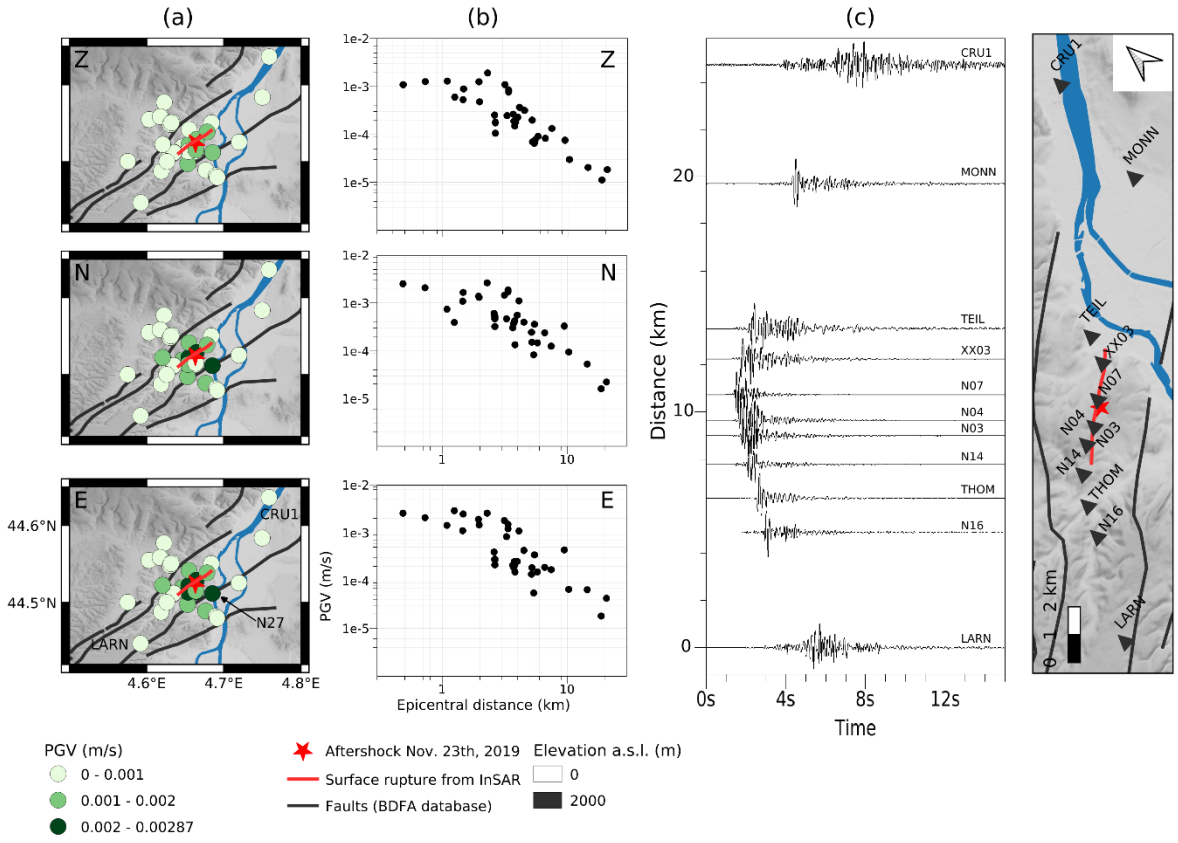
(a)
(b)
(c)
Z
N
E
CRU1
N27
LARN
44.6°N
44.5°N
4.6°E
4.7°E
4.8°E
1e-2
1e-3
1e-4
1e-5
1
10
PGV (m/s)
Epicentral distance (km)
Distance (km)
20
10
0
0s
4s
8s
12s
Time
MONN
TEIL
XX03
N07
N04
N03
N14
THOM
N16
0 1 2 km
PGV (m/s)
0 - 0.001
0.001 - 0.002
0.002 - 0.00287
Aftershock Nov. 23th, 2019
Surface rupture from InSAR
Faults (BDFA database)
Elevation a.s.l. (m)
0
2000

Fig. 10

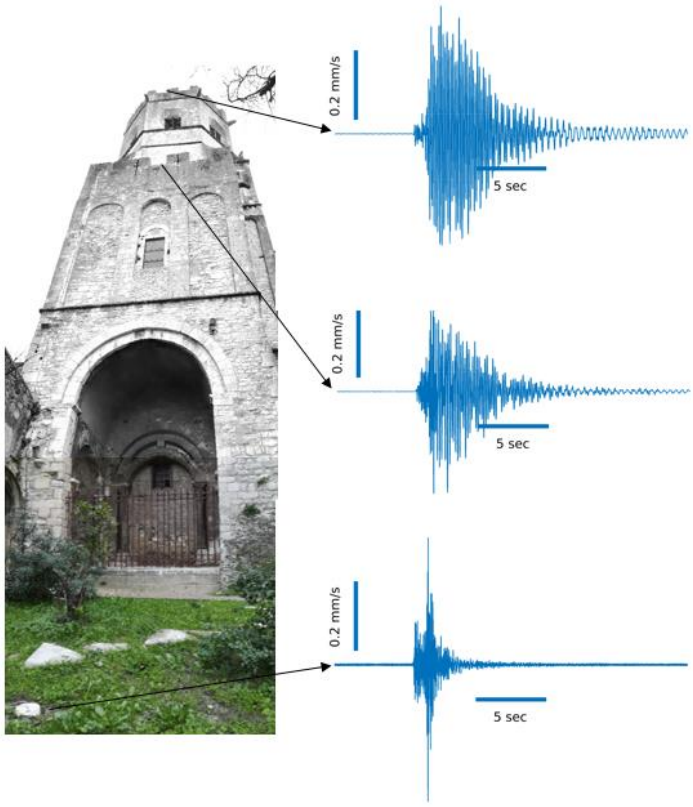

Fig. 11